Published in final edited form as:

J Orthop Res. 2023 October ; 41(10): 2238–2249. doi:10.1002/jor.25590.

Investigating the Temporal Roles of Decorin and Biglycan in Tendon Healing

Thomas P. Leahy[1,2,†], **Ashley K. Fung**[1,2,†], **Stephanie N. Weiss**[1], **Nathaniel A. Dyment**[1,2], **Louis J. Soslowsky**[1,2,*]

[1]McKay Orthopaedic Laboratory, University of Pennsylvania, Philadelphia, PA, USA

[2]Department of Bioengineering, University of Pennsylvania, Philadelphia, PA, USA

Abstract

The small leucine-rich proteoglycans, decorin and biglycan, are minor components of the tendon extracellular matrix that regulate fibrillogenesis and matrix assembly. Our study objective was to define the temporal roles of decorin and biglycan during tendon healing using inducible knockout mice to include genetic knockdown at specific phases of healing: time of injury, the proliferative phase, and the remodeling phase. We hypothesized that knockdown of decorin or biglycan would adversely affect tendon healing, and that by prescribing the timing of knockdown, we could elucidate the temporal roles of these proteins during healing. Contrary to our hypothesis, decorin knockdown did not affect tendon healing. However, when biglycan was knocked down, either alone or coupled with decorin, tendon modulus was increased relative to wild-type mice, and this finding was consistent among all induction timepoints. At 6 weeks post-injury, we observed increased expression of genes associated with the extracellular matrix and growth factor signaling in the biglycan knockdown and compound-decorin-biglycan knockdown tendons. Interestingly, these groups demonstrated opposing trends in gene expression as a function of knockdown-induction timepoint, highlighting distinct temporal roles for decorin and biglycan. In summary, this study finds that biglycan plays multiple functions throughout tendon healing, with the most impactful, detrimental role likely occurring during late-stage healing.

Statement of clinical importance: This study helps to define the molecular factors that regulate tendon healing, which may aid in the development of new clinical therapies.

Keywords

Tendon; Injury; Proteoglycan

[*]**Corresponding Author:** Louis J. Soslowsky, PhD, McKay Orthopaedic Research Laboratory, University of Pennsylvania, 307A Stemmler Hall, 3450 Hamilton Walk, Philadelphia, PA 19104-6081, T: 215-898-8653; F: 215-573-2133, soslowsk@upenn.edu, Twitter: @SoslowskyLab.

[†]indicates that authors contributed equally to this manuscript (i.e., co-first authors)

Author Contribution Statement: All authors contributed to the development of the study design, data interpretation, and manuscript editing. Data acquisition and analysis as well as manuscript drafting was performed by AKF and TPL. Mouse colony maintenance, mouse surgeries, and sample collection was performed SNW. All authors have read and approved the final manuscript for submission.

INTRODUCTION

Tendons transmit high tensile forces from muscle to bone via a hierarchically organized extracellular matrix (ECM). Tendon ECM consists primarily of collagen type I along with other minor collagens and proteoglycans, including the small leucine-rich proteoglycans (SLRPs), decorin (gene: *Dcn*) and biglycan (gene: *Bgn*). These SLRPs regulate collagen fibrillogenesis in tendon development by binding and stabilizing collagen I protofibrils to facilitate end-to-end and lateral growth.[1] Therefore, as expected, decorin and biglycan-null mice ($Dcn^{-/-}$ and $Bgn^{-/-}$, respectively) exhibit a severe aberrant phenotype in collagen fibril structure and organization.[2] Notably, genetic knockout of either SLRP altered fibril structure and increased viscoelastic mechanical properties in tendon.[3-7]

Clinical outcomes remain unsatisfactory following tendon injuries, which are common and debilitating. Therefore, there is a clinical need for increased understanding of the mechanisms that regulate tendon healing. Healing tendons follow a typical fibrotic wound healing pattern, including phases of inflammation, proliferation, and remodeling.[8] Previous studies found that decorin and biglycan regulate the tendon healing response to injury.[9,10] Specifically, mature (120 day old) $Bgn^{-/-}$ mice and $Dcn^{-/-}$ mice demonstrated attenuated early and late stage healing, respectively, with sustained reductions in dynamic modulus at 3 and 6 weeks post-injury compared to uninjured controls.[9]

While these studies implicate decorin and biglycan as regulators of tendon healing, the use of conventional knockout mouse models confounds whether attenuated healing in SLRP-deficient mice is impacted by pre-existing effects of SLRP deficiency during tendon development. To address this limitation in the present study, mice with a tamoxifen-inducible Cre-Lox system were used to conditionally knock down decorin and biglycan at specific phases of healing. Though decorin and biglycan are primarily known for their structural roles in tendon collagen fibrillogenesis and matrix assembly, these SLRPs can sequester as well as act as inflammatory and growth factor signaling molecules when released from the ECM.[11-14] This suggests that decorin and biglycan may have important cell functions to mediate inflammation and growth factor activity, thereby influencing collagen deposition, scar tissue formation, remodeling, and tendon function following injury. However, the temporal structural and biological roles of decorin and biglycan during tendon healing remain poorly understood.

Therefore, the first objective of this study (Study 1) was to define the regulatory roles of decorin and biglycan in tendon healing by inducing genetic knockdown of these SLRPs at the time of injury. Based on previous conventional knockout data,[9,10] we hypothesized that knockdown of decorin and biglycan would negatively impact tendon healing, with the compound *Dcn-Bgn* knockdown exhibiting the most pronounced negative effects on tendon healing. Our second objective (Study 2) was to investigate the *temporal* roles of decorin and biglycan in tendon healing by comparing the healing response when knockdown was induced during three healing phases: time of injury, proliferative phase, and remodeling phase. We hypothesized that reduced decorin expression would attenuate tendon healing similarly when knockdown was induced during early or late-stage healing, while biglycan

knockdown would demonstrate greater effects on healing when knockdown was induced during early rather than late-stage healing.

METHODS

Animal Use & Study Design

Animal use was approved by the University of South Florida and the University of Pennsylvania Institutional Animal Care and Use Committees. This study used 320 female mice divided between $Dcn^{+/+}/Bgn^{+/+}$ control (WT), $Dcn^{flox/flox}$ (I-$Dcn^{-/-}$), $Bgn^{flox/flox}$ (I-$Bgn^{-/-}$), and compound $Dcn^{flox/flox}/Bgn^{flox/flox}$ (I-$Dcn^{-/-}/Bgn^{-/-}$) mice with a tamoxifen (TM) inducible Cre (B6.129-Gt(ROSA)26Sortm1(cre/ERT2)Tyj/J, Jackson Labs).[15,16] Female mice were used because *Bgn* is located on the X chromosome. At 120 days old, mice underwent bilateral patellar tendon surgery to create excisional defects with a 0.75mm biopsy punch as described.[9,10,17-20] Cre excision was induced via two consecutive days of intraperitoneal injections of TM beginning on the day of surgery (50 mg/kg; T5648, Sigma-Aldrich, St. Louis, MO). In addition, uninjured WT control mice received the TM injection protocol beginning at 120 days old and were sacrificed 30 days later. All animals were randomly allocated into knockdown induction and sacrifice timepoints, and all assays were performed by a blinded investigator.

Study 1: To define the regulatory roles of decorin and biglycan in tendon healing, Cre excision of the targeted alleles was induced starting the day of injury (TM0), and mice were sacrificed 1, 3, or 6 weeks post-injury (Figure 1A). Patellar tendons were allocated for analysis of mechanical properties (3 & 6 weeks; n=16/group), tendon scar morphology (1, 3 & 6 weeks; n=4/group), collagen fibril ultrastructure (3 & 6 weeks; n=4/group), and gene expression (1, 3 & 6 weeks; n=4/group). All quantitative data was assessed for statistical outliers (defined as 2.2*IQR *a priori*). To evaluate the effects of genotype and healing timepoint, groups were compared with two-way ANOVAs with planned comparisons for mechanics, scar morphology, and fibril density. For collagen fiber realignment, genotypes within 3- and 6-week healing timepoints were compared with two-way ANOVAs (factors: genotype and strain value) with planned comparisons. For collagen fibril morphology, fibril diameter distributions were compared using Kolmogorov-Smirnov tests. For gene expression analyses, we performed separate non-parametric Kruskal-Wallis tests across healing timepoints within genotypes and across genotypes within healing timepoints. Subsequent Dunn-Sidak post-hoc tests for multiple comparisons were performed when necessary. Significance was set at $p \leq 0.05$ for all statistical analyses. Uninjured data was not included in the statistical analysis but is presented for context.

Study 2: The temporal roles of decorin and biglycan in tendon healing were investigated by inducing knockdown 5 days after injury (TM5; TM injections on days 5 and 6 post-injury) and 21 days after injury (TM21; TM injections on days 21 and 22 post-injury) (Figure 1B). The TM5 and TM21 knockdown induction timepoints were designed to be representative of the early proliferative and remodeling periods, respectively.[21-24] Data from Study 1 with knockdown induction at the time of injury (TM0; TM injections on the day of surgery and 1 day post-injury) was included in these comparisons. Animals were sacrificed at 3-weeks post-injury (TM5 only) and 6-weeks post-injury (TM5 and TM21), and patellar

tendons were allocated for assessment of mechanical properties (n=16/group), tendon scar morphology (n=4/group), collagen fibril ultrastructure (n=4/group), and gene expression (n=4/group). All quantitative data was assessed for statistical outliers (defined as 2.2*IQR *a priori*). Within each genotype and healing timepoint, induction timepoints along with the timepoint-matched WT group were compared using one-way ANOVAs with Tukey post-hoc tests (TM0 and TM5 for 3 weeks post-injury; TM0, TM5, and TM21 for 6 weeks post-injury) for mechanics, scar morphology, and fibril density data. For collagen fiber realignment data, groups at each healing timepoint were compared with a two-way ANOVA (factors: induction timepoint and strain value) with planned comparisons. Fibril diameter distributions were compared using Kolmogorov-Smirnov tests. Consistent with study 1, we analyzed our gene expression data across induction timepoints with non-parametric Kruskal-Wallis tests with subsequent Dunn-Sidak post-hoc tests for multiple comparisons. For all statistical analyses, significance was set at $p \leq 0.05$.

Tendon Scar Morphology

Knee joints were fixed in 10% neutral buffered formalin for 7 days, decalcified in 5% formic acid (Immunocal, Stat Labs) for 7 days, and processed for paraffin sectioning. Knees were sectioned in the transverse plane of the patellar tendon at a thickness of 10 μm. To minimize tissue shredding, the face of the block was soaked for 10 minutes in 5% fabric softener approximately every 200 μm while sectioning.[25,26] Sections were then stained with 0.1% toluidine blue. Scar tissue area was measured by a blinded investigator by manually outlining the entire tendon and the fibrotic scar (delineated by the increased cell density surrounding the excisional defect). Scar tissue area was calculated as a percent of the total tendon cross-sectional area.

Tendon Mechanics and Dynamic Collagen Fiber Realignment

Tibia-patellar tendon-patella complexes were dissected, and the patellar tendon was stamped to a width of 0.75 mm centered on the excisional defect. The stamped tendon cross-sectional area was measured using a custom laser device,[27] the tibia was potted in polymethyl methacrylate, and the tendon was mounted within a mechanical testing machine (5848, Instron; Norwood, MA). The mechanical testing protocol consisted of 10 cycles of preconditioning (sinusoidal oscillations with 0.5% strain amplitude centered at 1% strain), 5 minutes of recovery at 0% strain, and a quasi-static ramp to failure (0.1% strain per second). Linear modulus values were determined from the resulting stress-strain data. During the ramp to failure, collagen fiber realignment was measured through polarized light analysis as previously described.[28,29] Quantified realignment data, represented as circular variance, was normalized to the first discrete data point collected during the ramp to failure and extrapolated to generate data at 0% strain (i.e., normalized circular variance parameter will be greater than 1 at 0% strain). Realignment data was compared between groups at each integer macroscale strain value up to 6% strain, the maximum strain below which all samples failed.

Collagen Fibril Morphology

Patellar tendons were dissected, fixed in Karnovsky's fixative (4% paraformaldehyde, 2.5% glutaraldehyde, 0.1M sodium cacodylate, 8.0mM calcium chloride), post-fixed with

1% osmium tetroxide, dehydrated in ethanol, and embedded in Epon as described.[9,10,30] Transverse ultrathin sections (ranging from 80 to 100 nm) were acquired with an ultramicrotome, post-stained with UranyLess (EMS 22409) and 1% phosphotungstic acid, and imaged at 60,000x using a JEOL 1010 transmission electron microscope. Images were captured within the healing region, and collagen fibril diameters as well as fibril densities were measured using an automated custom software (MATLAB, Mathworks; Natick, MA).

Gene Expression

Patellar tendons were dissected immediately following euthanasia and stored in liquid nitrogen. Samples were later thawed in RNAlater-ICE (Invitrogen; Waltham, MA) and homogenized in TRIzol (Invitrogen; Waltham, MA). Using manufacturers' protocols, homogenized samples underwent RNA extraction (Direct-zol RNA Microprep, Zymo; Irvine, CA), cDNA reverse transcription (High Capacity cDNA RT, Thermo; Waltham, MA), and pre-amplification with selected probes (Taqman, Thermo; Waltham, MA). RNA quantity was normalized to 250 ng prior to cDNA conversion for all samples. RNA quality was evaluated for a subset of samples (24 out of 88 total samples, randomly divided among genotypes and experimental induction/sacrifice timepoints) via Agilent BioAnalyzer (RNA integrity number (RIN): 7.65±0.89 (mean±standard deviation)). Pre-amplified cDNA from all samples was loaded into a Fluidigm 96.96 Dynamic Array with Taqman assays to probe expression levels of 93 target genes relevant for tendon healing, including categories of collagens, non-collagenous matrix, matrix remodeling, cell-ECM proteins, and cell and inflammatory markers. Specific Taqman probes are listed in Supplemental Table 1. ΔCt was calculated by subtracting the gene Ct from average housekeeping Ct (*Abl1* and *Rps17*).

RESULTS

As expected, and consistent with previous homeostatic studies using these conditional tamoxifen-inducible mouse models,[15,16] we generally observed substantial knockdown of *Dcn* and *Bgn* expression in the relevant animal models used in this study (Figure 2). Two groups failed to achieve expected statistical significance compared to their corresponding healing timepoint-matched WT group: *Dcn* knockdown in the 3 week post-injury I-$Dcn^{-/-}/Bgn^{-/-}$ group ($p = 0.11$) and *Bgn* knockdown in the TM21 I-$Bgn^{-/-}$ group ($p = 0.34$). Importantly, we did not observe compensatory increases in gene expression in the opposite SLRP with *Dcn* or *Bgn* knockdown, which has been previously documented.[2,31]

Study 1: What are the roles of decorin and biglycan in tendon healing?

Knockdown of *Dcn* and *Bgn* did not affect scar morphology following injury.— In Study 1, we defined how knockdown of *Dcn* and/or *Bgn* at time of injury (i.e., TM0) altered the tendon healing response to injury. In histological sections of injured patellar tendons, there was significant healing scar tissue on the superficial side of the tendon defect that dissipated with increased time of healing (Figure 3A). As expected, scar area decreased with healing time in all groups, although there were no differences in scar area between genotypes at any healing timepoint (Figure 3B).

Bgn knockdown at time of injury increased tendon modulus at 6 weeks post-injury.—As expected, linear modulus was lower at 3 and 6 weeks post-injury relative to uninjured controls (Figure 3C). Interestingly, compound *Dcn-Bgn* knockdown (I-$Dcn^{-/-}/Bgn^{-/-}$) tendons had a greater modulus relative to WT and *Dcn* knockdown (I-$Dcn^{-/-}$) tendons at 3 weeks post-injury. At 6 weeks post-injury, *Bgn* knockdown (I-$Bgn^{-/-}$) and I-$Dcn^{-/-}/Bgn^{-/-}$ tendons had increased modulus relative to WT tendons. With loading, I-$Bgn^{-/-}$ tendons exhibited reduced collagen fiber realignment relative to WT and I-$Dcn^{-/-}$ tendons at 3 weeks post-injury (Figure 4A), although these differences were not present at 6 weeks post-injury (Figure 4B). Collectively, increased linear modulus in I-$Bgn^{-/-}$ and I-$Dcn^{-/-}/Bgn^{-/-}$ tendons suggests improved healing relative to WT and I-$Dcn^{-/-}$ tendons.

Bgn knockdown resulted in a narrower distribution of smaller collagen fibril diameters.—To further investigate the mechanisms underlying the increased moduli observed in *Bgn* knockdown (I-$Bgn^{-/-}$) and compound *Dcn-Bgn* knockdown (I-$Dcn^{-/-}/Bgn^{-/-}$) tendons, collagen fibril morphology within the healing region was evaluated using transmission electron microscopy. Although there were no differences between groups in collagen fibril density (Supplemental Figure 1A), fibril diameter distributions from I-$Bgn^{-/-}$ and I-$Dcn^{-/-}/Bgn^{-/-}$ tendons differed from those of WT and I-$Dcn^{-/-}$ tendons at both 3 and 6 weeks post-injury (Figure 5A,B). Specifically, fibril diameter distributions of I-$Bgn^{-/-}$ and I-$Dcn^{-/-}/Bgn^{-/-}$ tendons were narrower compared to WT and I-$Dcn^{-/-}$ tendons at both healing timepoints, indicating a more homogenous distribution. In addition, fibril diameter distributions of I-$Dcn^{-/-}/Bgn^{-/-}$ tendons were consistently skewed towards smaller diameter fibrils relative to other groups. Taken together with the linear modulus results, collagen fibril diameter distributions further suggest an altered healing mechanism in I-$Bgn^{-/-}$ and I-$Dcn^{-/-}/Bgn^{-/-}$ tendons compared to WT tendons.

Compound _Dcn-Bgn_ knockdown increased expression of healing related genes at 6 weeks post-injury.—We next explored the underlying biological response by measuring the expression of 93 genes implicated in tendon healing. As expected, tendon injury transiently upregulated many genes, including collagens and inflammatory genes compared to uninjured tendons (Figure 6A-D, Supplemental Figure 2). At 1 and 3 weeks post-injury, there were few differences in gene expression patterns between genotypes. Surprisingly, the most pronounced effects of SLRP knockdown occurred at the 6-week healing timepoint in I-$Dcn^{-/-}/Bgn^{-/-}$ tendons. For example, although there were no differences in *Col1a2* expression between genotypes at earlier timepoints, *Col1a2* expression was significantly increased at 6 weeks post-injury in the I-$Dcn^{-/-}/Bgn^{-/-}$ group compared to WT (Figure 6A). Further, while all other genotypes demonstrate reduced *Col1a2* expression by 6 weeks post-injury relative to either 1 or 3-weeks post-injury, this reduction was not observed in I-$Dcn^{-/-}/Bgn^{-/-}$ tendons (Figure 6A). Interestingly, I-$Dcn^{-/-}/Bgn^{-/-}$ tendons demonstrated similar expression patterns (i.e., increased expression relative to other groups at 6 weeks post-injury and/or attenuated decreases in expression over time) in several ECM-related genes, including collagens (*Col1a1*, *Col3a1*, and *Col6a1*, and *Col11a1;* Figure 6A), non-collagenous matrix proteins (*Eln*, *Fbn1*, *Fbn2*, and *Fmod*; Figure 6B), and matrix remodeling proteins (*Adamts2*, *Atamts5*, *Loxl2*, and *Mmp14*; Figure 6C). Finally, expression levels for many growth factor genes, including *Bmp2*, *Igf1*, *Mtor*,

Pdgfa, *Pdgfb*, *Tgfb3*, and *Vegfb*, were also upregulated in I-*Dcn*$^{-/-}$/*Bgn*$^{-/-}$ tendons at 6 weeks post-injury relative to other groups (Figure 6D). In summary, *Dcn-Bgn* knockdown alters the expression patterns of healing-related genes following tendon injury with the most pronounced effects during later stages.

Study 2: What are the temporal roles of decorin and biglycan in tendon healing?

Biglycan knockdown increased healing tendon modulus regardless of knockdown induction timepoint.—In Study 2, we evaluated how timing of *Dcn* and *Bgn* knockdown regulates the genotype-specific healing responses by comparing healing outcomes between knockdown induction at the time of injury (TM0; data from Study 1) to knockdown induction at 5 and 21 days post-injury (TM5 and TM21, respectively). Quantified scar area was not different between induction timepoints in any genotype at 3 or 6 weeks post-injury (Figure 7A-B). Mechanical testing analysis revealed an increased modulus in the TM5 *Bgn* knockdown (I-*Bgn*$^{-/-}$) group as well as the TM0 and TM5 compound *Dcn-Bgn* knockdown (I-*Dcn*$^{-/-}$/*Bgn*$^{-/-}$) groups relative to WT at 3 weeks post-injury (Figure 7C). At 6 weeks post-injury, I-*Bgn*$^{-/-}$ tendon modulus was increased relative to WT, regardless of induction timepoint (Figure 7D). Collagen fiber realignment was reduced in the TM5 I-*Bgn*$^{-/-}$ group relative to the WT and TM0 I-*Bgn*$^{-/-}$ groups at 3 weeks post-injury (Supplemental Figure 3A-C). At 6 weeks post-injury, fiber realignment was reduced in the TM5 *Dcn* knockdown (I-*Dcn*$^{-/-}$) and TM5 I-*Bgn*$^{-/-}$ groups compared to WT and their respective TM0 groups (Supplemental Figure 3D-F). Finally, collagen fibril diameter distributions exhibited subtle differences between induction timepoints in all groups (Figure 7E-F). Interestingly, fibril density was increased in TM5 I-*Bgn*$^{-/-}$ tendons relative to TM0 I-*Bgn*$^{-/-}$ tendons at 3 weeks post-injury (Supplemental Figure 1B), although there were no differences between groups at 6 weeks post-injury (Supplemental Figure 1C). In summary, mechanical analysis suggested improved healing in I-*Bgn*$^{-/-}$ tendons at 6 weeks post-injury, regardless of knockdown timepoint. In addition, subtle differences between induction timepoints in collagen fiber realignment and fibril diameter distributions suggest that decorin and biglycan have temporally specific roles throughout the phases of tendon healing.

Gene expression in healing I-*Bgn*$^{-/-}$ and I-*Dcn*$^{-/-}$/*Bgn*$^{-/-}$ tendons depends on knockdown induction timepoint.—Finally, we explored the effect of *Dcn* and *Bgn* knockdown timing on gene expression patterns. Consistent with our previous data, there were few differences in gene expression patterns between groups at 3 weeks post-injury (Supplemental Figure 4), while the most pronounced effects of *Dcn* and *Bgn* knockdown on gene expression occurred at 6 weeks post-injury (Figure 8A-D, Supplemental Figure 5). As in Study 1, the TM0 compound I-*Dcn*$^{-/-}$/*Bgn*$^{-/-}$ group demonstrated increased expression of many ECM-related and growth factor genes relative to WT tendons (Figure 8A-D). Interestingly, in I-*Dcn*$^{-/-}$/*Bgn*$^{-/-}$ tendons, the TM21 group exhibited reduced expression of many ECM-related and growth factor genes relative to the TM0 group, including *Col1a1*, *Col1a2*, *Col6a1*, *Col11a1*, *Fmod*, *Mmp3*, and *Pdgfa* (Figure 8A-D). Gene expression patterns in the TM5 I-*Dcn*$^{-/-}$/*Bgn*$^{-/-}$ group served as an intermediate between the TM0 and TM21 I-*Dcn*$^{-/-}$/*Bgn*$^{-/-}$ groups, as these genes were often not increased relative to WT nor reduced relative to the TM0 I-*Dcn*$^{-/-}$/*Bgn*$^{-/-}$ group (Figure 8A-D). The effect is not

necessarily surprising, as *Dcn* and *Bgn* knockdown for a greater duration would be expected to lead to a greater effect on gene expression. However, the I-*Bgn*$^{-/-}$ group demonstrates the opposite trend across knockdown induction timepoints, as the gene expression profiles differ more drastically relative to WT with later knockdown induction relative to injury (i.e., in the TM5 and TM21 groups). These differences are most dramatic in non-collagenous matrix and matrix remodeling genes, including *Fmod*, *Thbs4*, *Tnc*, and *Mmp3* (Figure 8B-C), as well as growth factor genes, specifically *Bmp2*, *Igf1*, and *Tgfb3* (Figure 8D). Taken together, opposing gene expression patterns across knockdown timepoints between I-*Bgn*$^{-/-}$ and I-*Dcn*$^{-/-}$/*Bgn*$^{-/-}$ tendons may indicate an overlapping functional role for *Dcn* and *Bgn* in regulating healing,[32,33] which is altered in I-*Dcn*$^{-/-}$/*Bgn*$^{-/-}$ tendons but unaffected in I-*Bgn*$^{-/-}$ tendons.

DISCUSSION

The objective of this study was to investigate the temporal, regulatory roles of decorin and biglycan during tendon healing. Study 1 defined the tendon healing response in *Dcn* knockdown (I-*Dcn*$^{-/-}$), *Bgn* knockdown (I-*Bgn*$^{-/-}$), and compound *Dcn*-*Bgn* knockdown (I-*Dcn*$^{-/-}$/*Bgn*$^{-/-}$) mice when knockdown was induced at the time of injury. Study 2 investigated the temporal roles of decorin and biglycan in tendon healing by comparing the results of Study 1 (i.e., TM0) with the effects of knockdown induction at 5 and 21 days post-injury (TM5 and TM21, respectively). Contrary to our hypothesis, knockdown of decorin alone had little effect on the tendon healing response, regardless of when knockdown was induced. Surprisingly, biglycan knockdown, both alone and coupled with decorin knockdown, generated a substantial, potentially beneficial effect on tendon healing that was most pronounced at the 6 weeks post-injury timepoint.

In our previous study using 120 day old conventional knockout mice,[9] injured *Bgn*$^{-/-}$ and *Dcn*$^{-/-}$ tendons had reduced tendon mechanical properties compared to wild-type tendons at 3 weeks and 6 weeks post-injury, respectively, suggesting a sequential role for these proteins in healing. However, uninjured *Bgn*$^{-/-}$ and *Dcn*$^{-/-}$ tendons also had lower dynamic moduli compared to WT tendons,[9] confounding whether the altered healing outcomes in *Bgn*$^{-/-}$ and *Dcn*$^{-/-}$ tendons were due to an impaired tendon ECM prior to injury or an attenuated healing response following injury. Taken together with the few differences observed in healing I-*Dcn*$^{-/-}$ tendons in the present study, our results collectively suggest that *Dcn* expression may play a greater role in regulating tendon development relative to healing response. Moreover, the minimal effect of *Dcn* knockdown is not necessarily surprising, as *Dcn* expression has previously been shown to decrease post-injury,[34] which we also observe within the present study. Interestingly, in the present study, we observed increased linear moduli with *Bgn* knockdown (either alone or in tandem with *Dcn* knockdown), which conflicts with the detrimental effect on healing observed in conventional *Bgn*$^{-/-}$ mice.[9] These opposing findings suggest that *Bgn* expression has differential roles between developmental and healing contexts and underscore the importance of using inducible mouse models to minimize confounding developmental effects.[6,7]

Tendon healing follows a typical wound healing process, including an inflammatory response to the acute injury followed by a proliferative phase, where resident tendon

fibroblasts and progenitor cells proliferate and deposit scar tissue to bridge the wound site.[8,24,35-37] Healing then progresses to the remodeling phase, where fibrillar collagens organize and crosslink along the longitudinal tendon axis. In the present study, *Bgn* knockdown generated the most pronounced effects on mechanical properties and gene expression at 6 weeks post-injury. Moreover, the increased mechanical properties observed in the I-$Bgn^{-/-}$ tendons were not affected by the knockdown timepoint. Taken together, our findings indicate that, compared to decorin, biglycan plays a more substantial role in tendon healing by negatively impacting late-stage tendon mechanical properties and healing-related gene expression. Interestingly, we observed differential responses to knockdown induction timepoints between I-$Bgn^{-/-}$ and I-$Dcn^{-/-}/Bgn^{-/-}$ tendons. Specifically, gene expression differences at 6 weeks post-injury were more pronounced with later knockdown in *Bgn* knockdown tendons and more pronounced with earlier knockdown in compound *Dcn-Bgn* knockdown tendons, which may suggest overlapping functions of decorin and biglycan and that functional compensation may occur in single knockdown models.[32,33]

The tendon healing response is often compared to tendon development, as both physiologically processes require coordinated synthesis, deposition, and remodeling of collagenous ECM. Fibrillogenesis is initiated by cellular synthesis and secretion of collagen protofibrils followed by fibril assembly via end-to-end and lateral association of protofibrils.[1] Subsequently, the ECM undergoes maturation through continued lateral growth of the fibrils as well as lysyl oxidase-mediated cross-linking and fibril stabilization via association with additional ECM proteins, including decorin and biglycan.[1] Given that *Bgn* knockdown appeared to have the greatest effect on late stage tendon healing, biglycan may similarly regulate late stage fibrillogenesis during tendon developmental and healing processes. Similar regulatory roles for these SLRPs in regulating late stage fibrillogenesis have been observed in the cornea, where compound decorin/biglycan-null mice demonstrate normal fibril organization at postnatal day 4 (P4), but largely aberrant fibril structure and organization with increased postnatal development at P60.[2]

While the structural roles of decorin and biglycan as regulators of fibrillogenesis and matrix assembly are well established,[1,2] their biological roles in tendon healing remain undefined. Although previous studies have demonstrated that decorin and biglycan regulate inflammatory signaling by acting as agonists of toll-like receptors-2 and −4 to promote the release of pro-inflammatory cytokines,[11,38,39] we observed only minor differences in gene expression of inflammatory markers with SLRP knockdown. In addition to inflammatory cytokine signaling, many growth factors, such as the transforming growth factor β (TGF-β) family, are upregulated following injury and can promote profibrotic processes and tissue fibrosis.[40-43] Interestingly, decorin and biglycan bind TGF-β *in vitro* and may regulate the fibrotic response to injury by sequestering TGF-β in the ECM.[13,14] Though we did not observe differences in fibrotic scar tissue area between groups, gene expression data indicates increased expression of growth factors in TM0 *I-*$Dcn^{-/-}/Bgn^{-/-}$ tendons at 6 weeks post-injury. Specifically, there was increased expression of *Tgfb1* and *Tgfb3*, which may be driving increased collagenous and non-collagen matrix gene expression.[44]

In this study, we observed increased linear moduli in I-$Bgn^{-/-}$ and I-$Dcn^{-/-}/Bgn^{-/-}$ tendons relative to other groups, although these tendons were not drastically different from other

genotypes histologically. In addition, the narrower and smaller collagen fibril diameter distributions of I-*Bgn*$^{-/-}$ and I-*Dcn*$^{-/-}$/*Bgn*$^{-/-}$ tendons differed from the heterogeneous bimodal distribution observed in uninjured tendons, indicating that an expedited return to uninjured fibril structure is not driving increased mechanical properties. Additionally, increased expression of ECM-related genes in I-*Bgn*$^{-/-}$ and I-*Dcn*$^{-/-}$/*Bgn*$^{-/-}$ tendons at 6 weeks post-injury supports the increased mechanical properties and may also indicate a role for the non-collagenous matrix in driving genotype-specific healing outcomes. Ultimately, the underlying factor driving increased moduli in I-*Bgn*$^{-/-}$ and I-*Dcn*$^{-/-}$/*Bgn*$^{-/-}$ tendons remains unknown. For example, it may be that the altered mechanical, fiber realignment, and gene expression findings are indicative of a pathological fibrotic response. In line with this interpretation, reduced fiber realignment in I-*Bgn*$^{-/-}$ tendons at 3 weeks post-injury may indicate that the deposited healing matrix is less functional. However, due to differences in length scales and injury region-specificity of our fibril (TEM) and fiber scale (polarized light) analyses, we cannot decipher whether this decreased fiber realignment response is specific to the *de novo* healing ECM. Nevertheless, we argue that the differences in I-*Bgn*$^{-/-}$ and I-*Dcn*$^{-/-}$/*Bgn*$^{-/-}$ tendons likely represent an improved healing response rather than aberrant fibrosis, as there were no differences in fibrotic scar area. To further delineate the differential healing mechanisms observed in this study, additional mechanical analyses, including viscoelastic testing and/or measuring local properties of the injured scar, are needed. It is also important to note that our gene expression analysis was performed on the entire tendon and not the injury region due to technical limitations necessary for high RNA quality. In the future, techniques such as laser capture microdissection could be used to isolate the healing region.[45] Finally, unbiased gene expression analysis along with a comprehensive proteomics-based approach may also help to elucidate differences in healing mechanisms, particularly within the non-collagenous matrix.

In this study, we used a full-thickness, partial-width excisional defect of the patellar tendon, which we have demonstrated to be a very consistent injury model compared to similar incisional and excisional defects in the flexor digitorum longus or Achilles tendons.[9,10,17-20] This reproducible and excisional defect model is beneficial for evaluating *de novo* healing tendon ECM with attenuated genetic expression of *Dcn* and/or *Bgn*. We hypothesize that the fundamental roles of *Dcn* and *Bgn* in tendon healing established in this study would translate to other models, but further investigation within clinically-relevant injury models would account for different biochemical and biomechanical considerations.[46]

Finally, while inducible knockdown mouse models remove confounding developmental effects, *Dcn* and *Bgn* knockdown is less robust compared to conventional *Dcn*$^{-/-}$ and *Bgn*$^{-/-}$ knockout mouse models. Knockdown timing also generated variable knockdown efficiency, as induction at 21 days post-injury (TM21) led to reduced *Dcn* and *Bgn* knockdown relative to induction at time of injury and 5 days post-injury (TM0 and TM5, respectively). An additional limitation is that tamoxifen-induced Cre excision does not deplete existing decorin and/or biglycan proteins, which have a protein turnover half-life of 3 weeks or greater in the tendon ECM.[47] The combination of an excisional defect and techniques to specifically evaluate *de novo* ECM synthesized with reduced SLRP expression mitigates this limitation, and future proteomic analysis would be beneficial for quantifying decorin and biglycan protein content. Regardless, the use of this tamoxifen-inducible model is a

necessary and innovative approach to investigate the temporal roles of decorin and biglycan during different phases of healing, and our results showed that knockdown was sufficient to drive the development of unique phenotypes in the I-*Bgn*$^{-/-}$ and I-*Dcn*$^{-/-}$/*Bgn*$^{-/-}$ tendons at all induction timepoints, suggesting that the underlying tendon biological healing response was affected as needed for this study.

In conclusion, this study elucidates specific temporal roles of decorin and biglycan in tendon healing. While we found little effect of decorin knockdown on tendon healing, biglycan knockdown elicited a robust healing response, including increased linear modulus and expression of ECM-related and growth factor genes relative to WT tendons. Interestingly, timing of knockdown induction appeared to regulate the biological response (i.e., altered gene expression profiles) but did not overtly impact tendon healing outcomes. This suggests that while biglycan plays differential roles throughout healing, its most impactful role in restoring tendon mechanical properties occurs in late-stage healing. Future studies will investigate the specific mechanism by which biglycan regulates tendon healing by analyzing changes in tissue proteomics with *Bgn* knockdown and by uncovering the molecular binding partners of biglycan.

Supplementary Material

Refer to Web version on PubMed Central for supplementary material.

Acknowledgements:

This study was supported by the NIH/NIAMS (T32AR007132, R01AR068057) and the Penn Center for Musculoskeletal Disorders (P30AR069619). We thank Dr. David Birk for providing the mice and for his guidance and expertise as well as Sheila Adams for her assistance. We also acknowledge support from the University of Pennsylvania Electronic Microscopy Resource Lab and Molecular Profiling Facility Cores.

References

1. Chen S & Birk DE The regulatory roles of small leucine-rich proteoglycans in extracellular matrix assembly. FEBS J. 280, 2120–2137 (2013). [PubMed: 23331954]
2. Zhang G. et al. Genetic Evidence for the Coordinated Regulation of Collagen Fibrillogenesis in the Cornea by Decorin and Biglycan. J. Biol. Chem 284, 8888–8897 (2009). [PubMed: 19136671]
3. Robinson PS et al. Strain-Rate Sensitive Mechanical Properties of Tendon Fascicles from Mice with Genetically Engineered Alterations in Collagen and Decorin. J. Biomech. Eng 126, 252–257 (2004). [PubMed: 15179856]
4. Robinson PS et al. Influence of Decorin and Biglycan on Mechanical Properties of Multiple Tendons in Knockout Mice. J. Biomech. Eng 127, 181–185 (2005). [PubMed: 15868800]
5. Zhang G. et al. Decorin regulates assembly of collagen fibrils and acquisition of biomechanical properties during tendon development. J. Cell. Biochem 98, 1436–1449 (2006). [PubMed: 16518859]
6. Dourte LM et al. Influence of decorin on the mechanical, compositional, and structural properties of the mouse patellar tendon. J. Biomech. Eng 134, (2012).
7. Dourte LM et al. Mechanical, compositional, and structural properties of the mouse patellar tendon with changes in biglycan gene expression. J. Orthop. Res 31, 1430–1437 (2013). [PubMed: 23592048]
8. Velnar T, Bailey T & Smrkolj V The wound healing process: An overview of the cellular and molecular mechanisms. J. Int. Med. Res 37, 1528–1542 (2009). [PubMed: 19930861]

9. Dunkman AA et al. The Tendon Injury Response is Influenced by Decorin and Biglycan. Ann. Biomed. Eng 42, 619–630 (2014). [PubMed: 24072490]
10. Dunkman AA et al. The injury response of aged tendons in the absence of biglycan and decorin. Matrix Biol. 35, 232–238 (2014). [PubMed: 24157578]
11. Schaefer L. et al. The matrix component biglycan is proinflammatory and signals through Toll-like receptors 4 and 2 in macrophages. J. Clin. Invest 115, (2005).
12. Honardoust D. et al. Small leucine-rich proteoglycans, decorin and fibromodulin, are reduced in postburn hypertrophic scar. doi:10.1111/j.1524-475X.2011.00677.x
13. Kolb M, Margetts PJ, Sime PJ & Gauldie J Proteoglycans decorin and biglycan differentially modulate TGF-mediated fibrotic responses in the lung. (2001).
14. Hildebrand A. et al. Interaction of the small interstitial proteoglycans biglycan, decorin and fibromodulin with transforming growth factor β. Biochem. J 302, 527–534 (1994). [PubMed: 8093006]
15. Robinson KA et al. Decorin and biglycan are necessary for maintaining collagen fibril structure, fiber realignment, and mechanical properties of mature tendons. Matrix Biol. 64, 81–93 (2017). [PubMed: 28882761]
16. Beach ZM et al. Biglycan has a major role in maintenance of mature tendon mechanics. (2022). doi:10.1002/jor.25299
17. Beason DP, Kuntz AF, Hsu JE, Miller KS & Soslowsky LJ Development and Evaluation of Multiple Tendon Injury Models in the Mouse. J. Biomech 45, 1550 (2012). [PubMed: 22405494]
18. Mienaltowski MJ et al. Injury response of geriatric mouse patellar tendons. J. Orthop. Res 34, 1256–1263 (2016). [PubMed: 26704368]
19. Johnston JM et al. Collagen V haploinsufficiency in a murine model of classic Ehlers–Danlos syndrome is associated with deficient structural and mechanical healing in tendons. J. Orthop. Res 35, 2707–2715 (2017). [PubMed: 28387435]
20. Beach ZM, Fung AK, Weiss SN & Soslowsky LJ Post-injury tendon mechanics are not affected by tamoxifen treatment. 10.1080/03008207.2022.2097907 1–7 (2022). doi:10.1080/03008207.2022.2097907
21. Gonzalez ACDO, Andrade ZDA, Costa TF & Medrado ARAP Wound healing - A literature review. An. Bras. Dermatol 91, 614 (2016). [PubMed: 27828635]
22. Yang G, Rothrauff BB & Tuan RS Tendon and Ligament Regeneration and Repair: Clinical Relevance and Developmental Paradigm. doi:10.1002/bdrc.21041
23. Hope M & Saxby TS Tendon Healing. Foot Ankle Clin. 12, 553–567 (2007). [PubMed: 17996614]
24. Voleti PB, Buckley MR & Soslowsky LJ Tendon Healing: Repair and Regeneration. 10.1146/annurev-bioeng-071811-150122 14, 47–71 (2012).
25. Sharma P, Sharma S, Kaul Murthy S, Singal A & Grover C Comparison of four softening agents used on formalin-fixed paraffin-embedded nail biopsies with inflammatory disease. J. Histotechnol 43, 3–10 (2020). [PubMed: 31433736]
26. Porter A. et al. Quick and inexpensive paraffin-embedding method for dynamic bone formation analyses. Sci. Reports 2017 71 7, 1–7 (2017).
27. Favata M. Scarless healing in the fetus: Implications and strategies for postnatal tendon repair. Diss. available from ProQuest (2006).
28. Lake SP, Miller KS, Elliott DM & Soslowsky LJ Effect of fiber distribution and realignment on the nonlinear and inhomogeneous mechanical properties of human supraspinatus tendon under longitudinal tensile loading. J. Orthop. Res 27, 1596–1602 (2009). [PubMed: 19544524]
29. Miller KS, Connizzo BK, Feeney E & Soslowsky LJ Characterizing local collagen fiber re-alignment and crimp behavior throughout mechanical testing in a mature mouse supraspinatus tendon model. J. Biomech 45, 2061–2065 (2012). [PubMed: 22776688]
30. Birk DE & Trelstad RL Extracellular compartments in matrix morphogenesis: collagen fibril, bundle, and lamellar formation by corneal fibroblasts. J. Cell Biol 99, 2024 (1984). [PubMed: 6542105]

31. Ameye L & Young MF Mice deficient in small leucine-rich proteoglycans: novel in vivo models for osteoporosis, osteoarthritis, Ehlers-Danlos syndrome, muscular dystrophy, and corneal diseases. Glycobiology 12, 107R–116R (2002).
32. Corsi A. et al. Phenotypic Effects of Biglycan Deficiency Are Linked to Collagen Fibril Abnormalities, Are Synergized by Decorin Deficiency, and Mimic Ehlers-Danlos-Like Changes in Bone and Other Connective Tissues. (2002).
33. Wadhwa S. et al. Impaired posterior frontal sutural fusion in the biglycan/decorin double deficient mice. Bone 40, 861–866 (2007). [PubMed: 17188951]
34. Berglund M, Reno C, Hart DA & Wiig M Patterns of mRNA Expression for Matrix Molecules and Growth Factors in Flexor Tendon Injury: Differences in the Regulation Between Tendon and Tendon Sheath. J. Hand Surg. Am 31, 1279–1287 (2006). [PubMed: 17027787]
35. Dyment NA et al. The Paratenon Contributes to Scleraxis-Expressing Cells during Patellar Tendon Healing. PLoS One 8, 59944 (2013).
36. Dyment NA et al. Lineage Tracing of Resident Tendon Progenitor Cells during Growth and Natural Healing. PLoS One 9, (2014).
37. Dyment NA & Galloway JL Regenerative biology of tendon: mechanisms for renewal and repair. Curr. Mol. Biol. reports 1, 124 (2015).
38. Moreth K. et al. Biglycan-triggered TLR-2- and TLR-4-signaling exacerbates the pathophysiology of ischemic acute kidney injury. Matrix Biol. 35, 143–151 (2014). [PubMed: 24480070]
39. Merline R. et al. Signaling by the Matrix Proteoglycan Decorin Controls Inflammation and Cancer through PDCD4 and microRNA-21. Sci. Signal 4, ra75 (2011). [PubMed: 22087031]
40. Serini G. et al. The fibronectin domain ED-A is crucial for myofibroblastic phenotype induction by transforming growth factor-beta1. J. Cell Biol 142, 873–881 (1998). [PubMed: 9700173]
41. Sime PJ, Xing Z, Graham FL, Csaky KG & Gauldie J Adenovector-mediated gene transfer of active transforming growth factor-beta1 induces prolonged severe fibrosis in rat lung. J. Clin. Invest 100, 768–776 (1997). [PubMed: 9259574]
42. Lodyga M. et al. Cadherin-11–mediated adhesion of macrophages to myofibroblasts establishes a profibrotic niche of active TGF-. Sci. Signal 12, 3469 (2019).
43. Wipff PJ, Rifkin DB, Meister JJ & Hinz B Myofibroblast contraction activates latent TGF-beta1 from the extracellular matrix. J. Cell Biol 179, 1311–1323 (2007). [PubMed: 18086923]
44. Klein MB, Yalamanchi N, Pham H, Longaker MT & Chang J Flexor tendon healing in vitro: Effects of TGF-β on tendon cell collagen production. J. Hand Surg. Am 27, 615–620 (2002). [PubMed: 12132085]
45. Tsinman TK et al. Intrinsic and growth-mediated cell and matrix specialization during murine meniscus tissue assembly. FASEB J. 35, e21779 (2021). [PubMed: 34314047]
46. Theodossiou SK & Schiele NR Models of tendon development and injury. BMC Biomed. Eng 1, (2019).
47. Choi H. et al. Heterogeneity of proteome dynamics between connective tissue phases of adult Tendon. Elife 9, 1–22 (2020).

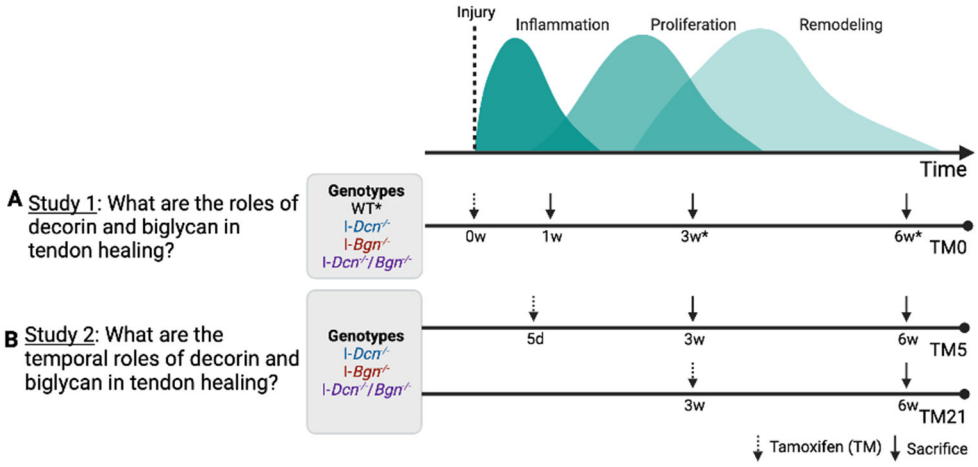

Figure 1. Overall study design.

Induction timepoints were chosen to target three temporal phases of tendon healing. (A) In Study 1, tamoxifen (TM) was administered at time of injury (TM0), and mice were sacrificed at 1, 3, or 6 weeks post-injury. (B) In Study 2, tamoxifen was injected at 5 or 21 days post-injury (TM5 and TM21, respectively), and mice were sacrificed at 3- (TM5) and 6-weeks (TM5 & TM21) post-injury. *indicates data is also included in Study 2 statistical comparisons.

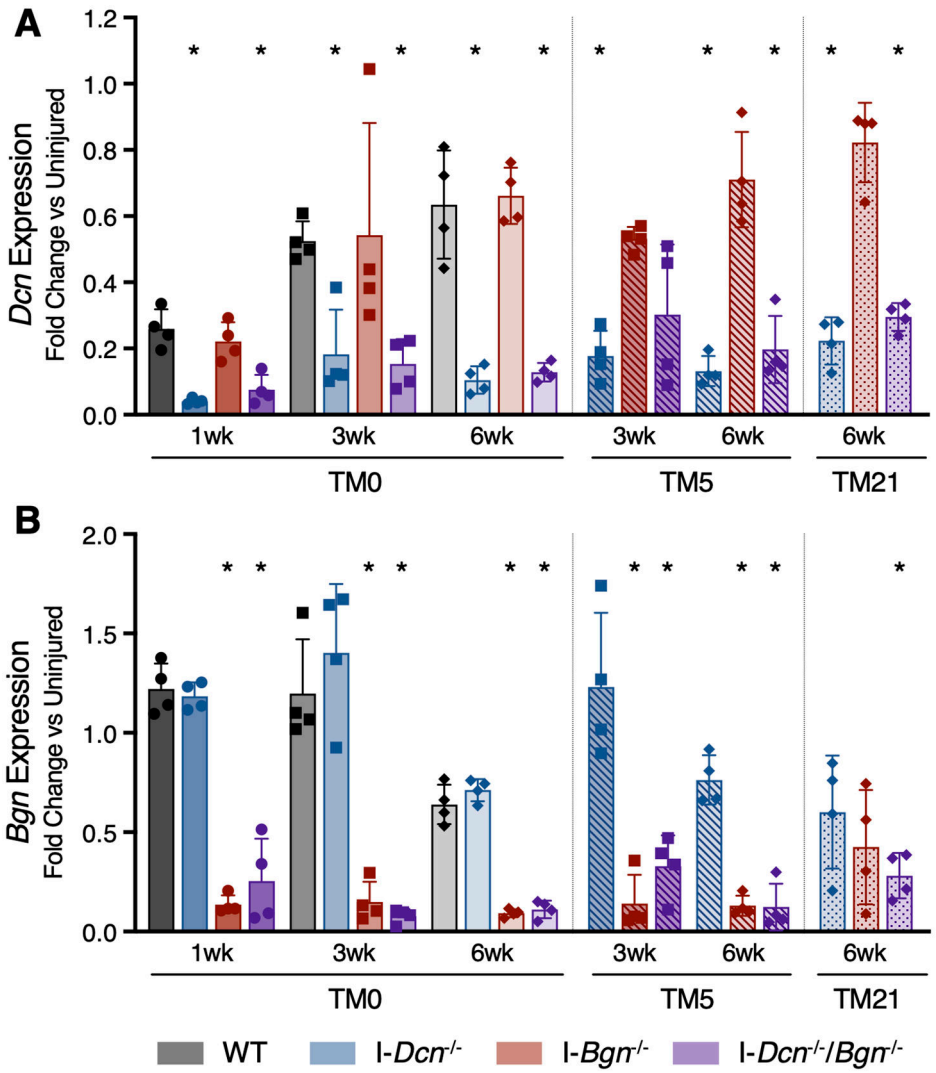

Figure 2. Gene expression of *Dcn* and *Bgn* knockdown.

As expected, the RosaCre-ER^{T2} conditional models achieved substantial *Dcn* and *Bgn* knockdown across all healing and induction timepoints. Data is represented as fold change relative to WT uninjured values ($2^{\Delta\Delta Ct}$, where $\Delta\Delta Ct = \Delta Ct_{sample} - \Delta Ct_{uninjured}$). * indicates significant difference ($p \leq 0.05$) from the corresponding healing timepoint-matched WT group via non parametric Mann-Whitney tests.

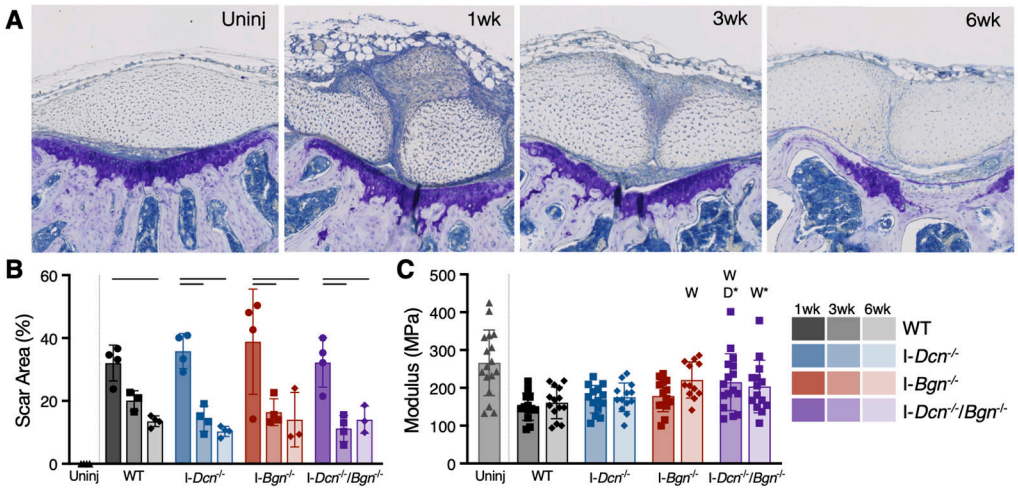

Figure 3. Tendon morphology and mechanics (Study 1).

(A) Transverse sections of uninjured and injured patellar tendons were stained with toluidine blue to quantify (B) scar area as a percentage of cross-sectional area at 1, 3, and 6 weeks post-injury. Scar area percentage decreased during healing, but no genotype differences were observed. (C) Modulus of I-*Bgn*$^{-/-}$ tendons was higher at 6 weeks post-injury and at both 3 and 6 weeks post-injury in the I-*Dcn*$^{-/-}$/*Bgn*$^{-/-}$ group compared to WT. Data is plotted as mean ± standard deviation. ‘W’ and ‘D’ indicate significant differences from WT and I-*Dcn*$^{-/-}$, respectively with * denoting p≤0.1.

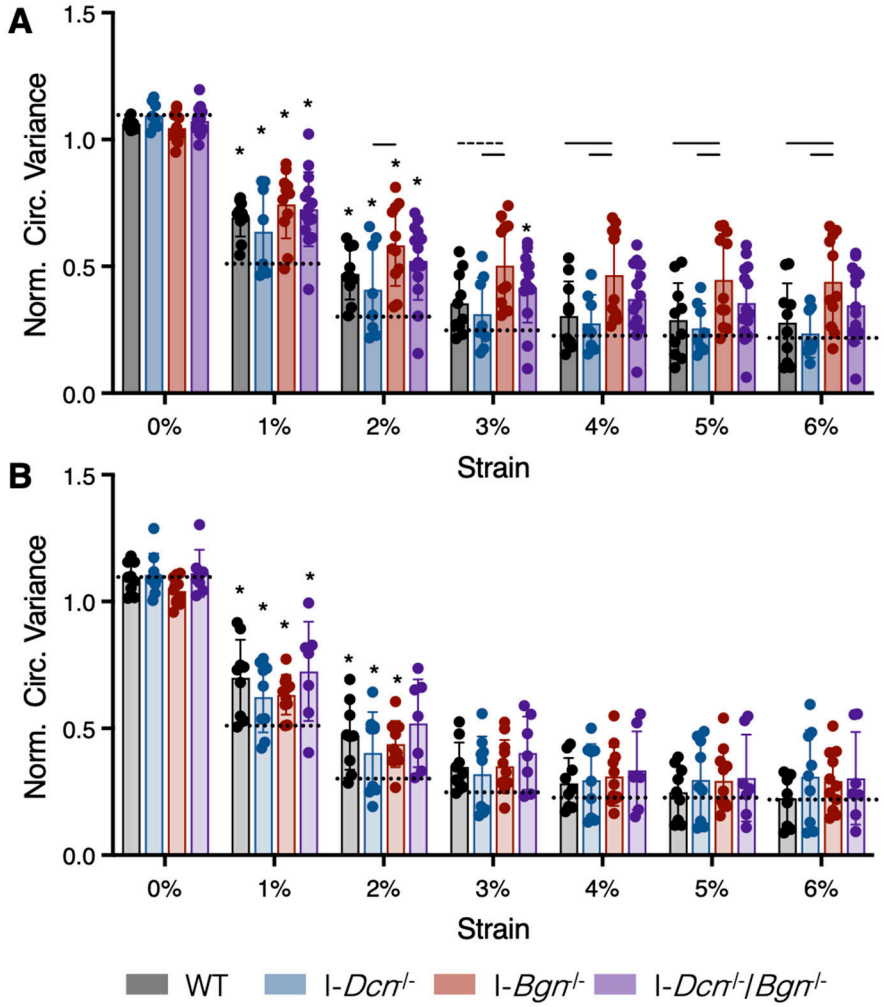

Figure 4. Collagen fiber realignment (Study 1).

(A) At 3 weeks post-injury, reduced collagen fiber realignment was observed in I-*Bgn*$^{-/-}$ tendons compared to WT and I-*Dcn*$^{-/-}$ tendons, while no differences between genotypes were observed at (B) 6 weeks post-injury. Data is represented as circular variance normalized to the first discrete data point, and data is plotted as mean ± standard deviation. Significant differences ($p \leq 0.05$) between genotypes are represented by solid lines, while '*' indicates a significant difference from its prior strain value.

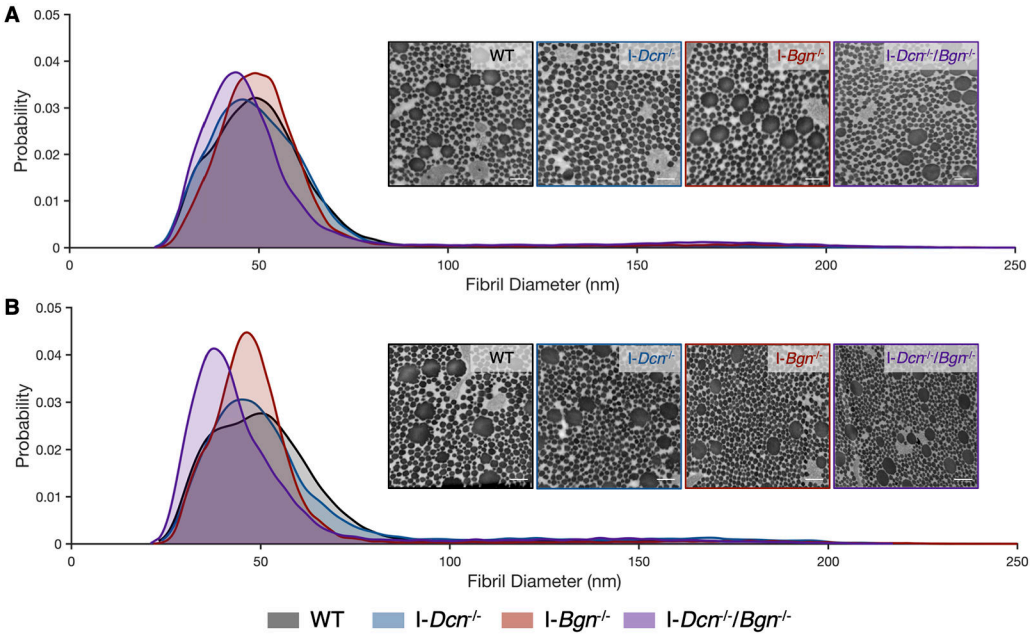

Figure 5. Collagen fibril ultrastructure (Study 1).

Probability density plots of collagen fibril diameters at 3 (A) and 6 (B) weeks post-injury demonstrated more homogenous distributions of collagen fibril diameters in the I-$Bgn^{-/-}$ and I-$Dcn^{-/-}/Bgn^{-/-}$ groups. Scale bar = 200nm.

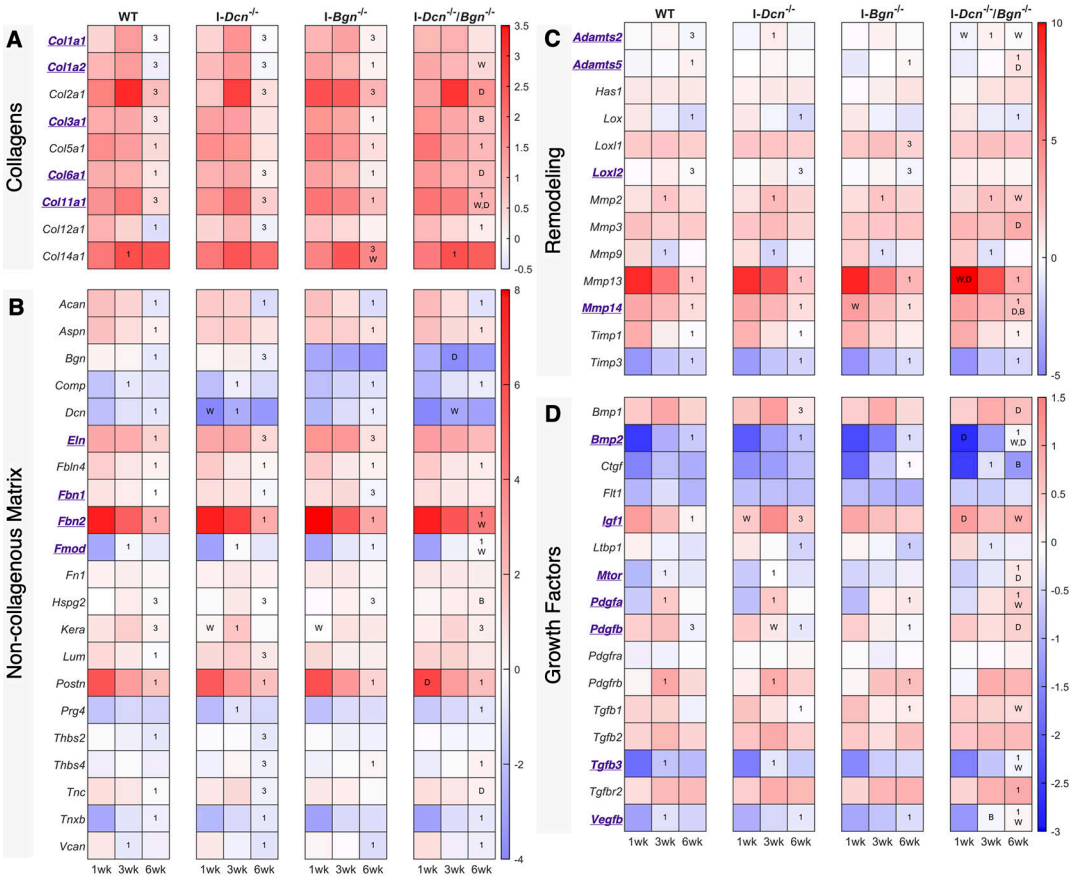

Figure 6. Gene expression (Study 1).

Gene expression data for A) collagens, B) non-collagenous matrix molecules, C) remodeling proteins, and D) growth factors generally demonstrated increased expression levels in the I-*Dcn*$^{-/-}$/*Bgn*$^{-/-}$ tendons at 6 weeks post-injury relative to other genotypes. All data is normalized to uninjured controls (represented as $\Delta\Delta Ct = Ct_{sample} - Ct_{uninjured}$). Genes that are referred to in the text are highlighted in purple. '1' and '3' indicate significant differences from the 1 and 3 week post injury timepoints, respectively. 'W', 'D', and 'B' indicate significant differences from WT, I-*Dcn*$^{-/-}$, and I-*Bgn*$^{-/-}$ groups, respectively.

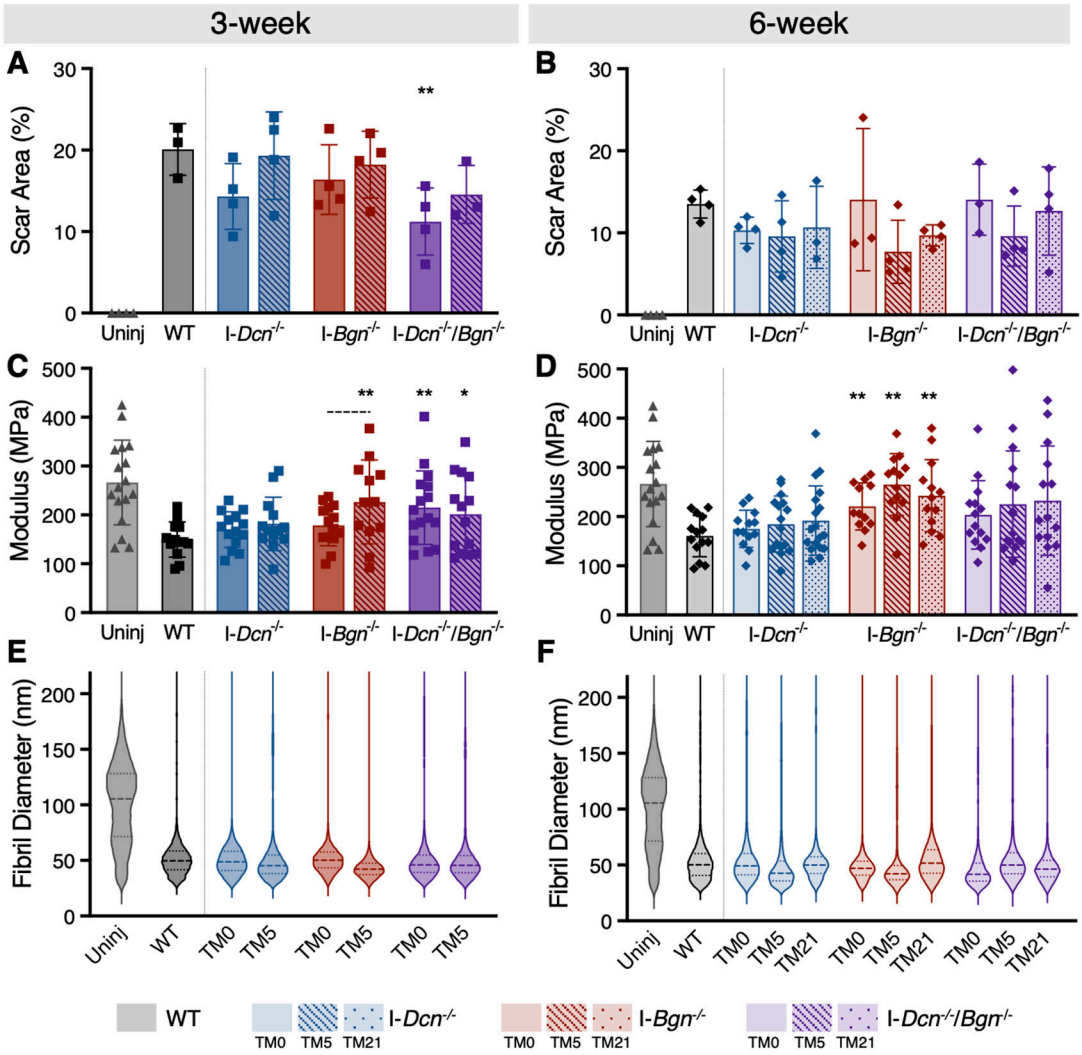

Figure 7. Tendon morphology, mechanics, and fibril ultrastructure (Study 2).

There were no differences in quantified scar area between knockdown induction timepoints at (A) 3 weeks or (B) 6 weeks post-injury. (C) Modulus was increased compared to WT tendons in I-$Bgn^{-/-}$ and I-$Dcn^{-/-}/Bgn^{-/-}$ tendons when knockdown was induced 5 days post-injury (TM5). (D) At 6 weeks post-injury, the modulus of I-$Bgn^{-/-}$ tendons was elevated compared to WT at all induction timepoints. All injured collagen fibril distributions were drastically different from the bimodal distribution observed in uninjured tendons. (E) No remarkable differences were observed at 3 weeks post-injury between induction timepoint, (F) but there was a noticeable shift in the collagen fibril distribution of I-$Bgn^{-/-}$ tendons when knockdown was induced 21 days post-injury (TM21) with a greater percentage of larger diameter fibrils. **‘**’** indicates significant difference from timepoint-matched WT group, while ‘*’ and dashed lines denote trends ($p \leq 0.1$).

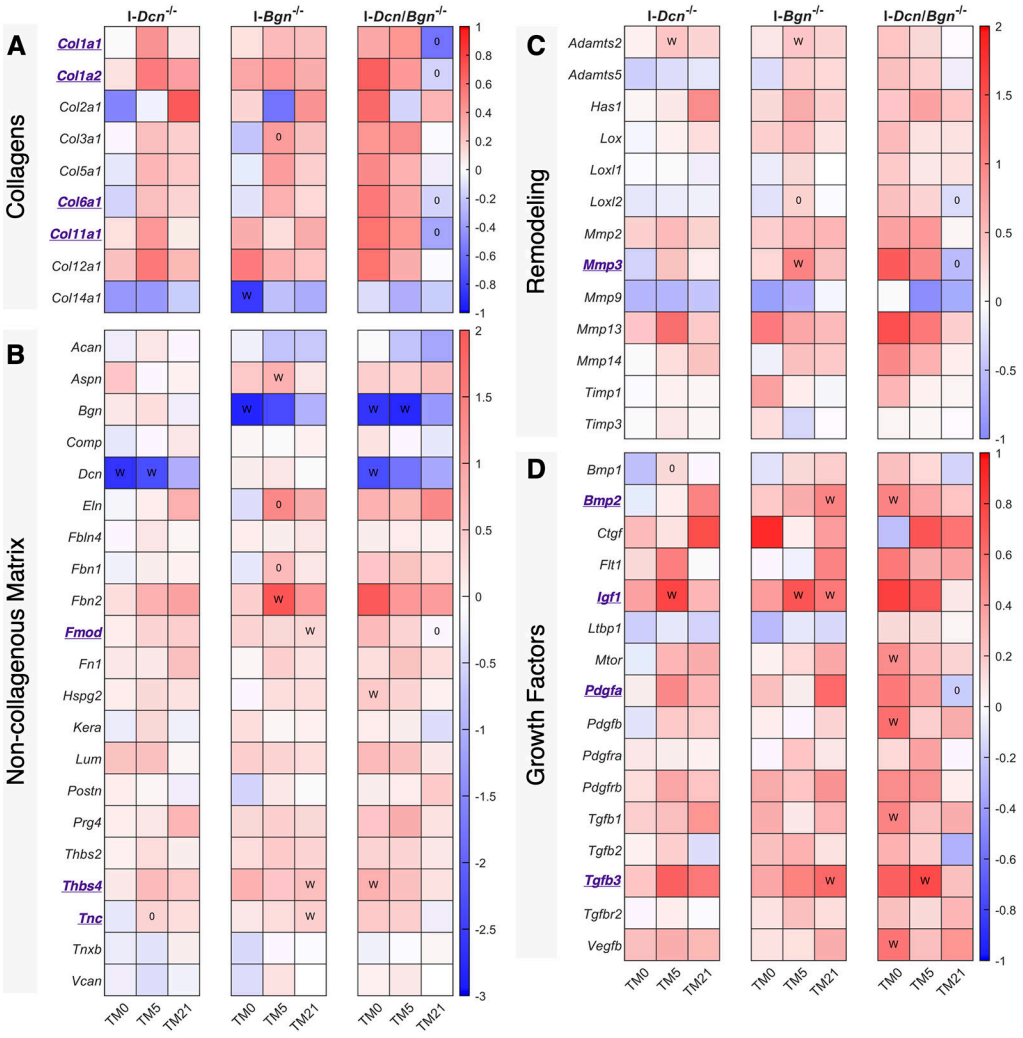

Figure 8. Gene expression at 6 weeks post-injury (Study 2).

Gene expression data for A) collagens, B) non-collagenous matrix molecules, C) remodeling proteins, and D) growth factors generally demonstrated opposing trends across knockdown induction timepoints in I-*Bgn*$^{-/-}$ and I-*Dcn*$^{-/-}$/*Bgn*$^{-/-}$ tendons at 6 weeks post-injury. All data is normalized to 6-week post-injury WT group (represented as $\Delta\Delta Ct = Ct_{sample} - Ct_{WT}$). '0' indicates significant differences from the TM0 group. 'W' from the 6-week post-injury WT group.